OVERPOWER BURNOUT

STANDARD PROBLEM NO. 4

ANALYSIS OF SINGLE FUEL ROD BEHAVIOR FOLLOWING CHF DUE TO OVERPOWER - POWER BURST FACILITY TEST SERIES PCM-20.

JUL 10 1973

OVERPOWER BURNOUT

Standard Problem Number 4

Introduction

The Power Burst Facility (PBF) has recently achieved criticality and is now ready to undertake a broad range of fuel behavior experimental investigations ranging through all postulated LWR accidents involving fuel. Included in the intended program for the PBF are tests of fuel behavior during the Loss-of-Coolant Accident (LOCA), various Power-Coolant Mismatch (PCM) accidents (such as overpower, loss of flow and flow blockage), and Reactivity Initiated Accidents (RIA). A preliminary (draft) description of the PBF program, ANCR-1012, is available which describes many of the details of these experiments.

First among the experiments planned for the PBF is test series PCM-20 which addresses the problem of overpower and behavior of fuel rods after CHF has been established. The preliminary experimental plans for this test series are contained in the Detailed Test Plan Report (DTPR). Because data from the PCM-20 experiments will soon be available, it is appropriate that a suitable portion of this overpower fuel behavior problem be established as a Standard Problem. The following pages provide a first look at this Standard Problem.

PBF Program Objectives

The objective of the experimental program planned for the Power Burst Facility is to gain an improved understanding of the behavior of reactor fuels during a range of postulated accidents. This is to be accomplished through a coordinated analytical and experimental effort which first develops models of LWR fuel behavior and subsequently, verifies these models via experimental data. The process consists basically of 4 steps.

1. First a simplified model is developed on basic theoretical considerations which includes a first order representation of known effects.
2. A series of tests are run with small test samples (single rods) to confirm that the model is complete; ie, that no major consideration has been omitted. On the basis of the data obtained from these tests, the model is modified as required to include the treatment of empirically observed effects.
3. Additional tests are run with the larger test assemblies to confirm that the models adequately account for the interactions between the various events being modeled.
4. The improved understanding of the fuel behavior phenomena and the data obtained from testing will be used to evaluate and improve the analytical methods for predicting fuel behavior in full-scale reactors subjected to hypothetical accidents.

Power-Cooling Mismatch

A number of abnormal reactor conditions have been postulated that could result in an imbalance between the heat generation rate in the fuel and the heat removal capacity of the coolant. This imbalance, termed a power-cooling mismatch (PCM) accident can arise in a reactor either from an overpower or undercooling situation, or a combination of these. The fuel rod behavior which follows PCM initiation is basically dependent upon whether the critical heat flux (CHF) for the local power and coolant conditions is surpassed. If CHF is not surpassed, the fuel and cladding temperatures will remain at or near their normal operating values. If CHF is surpassed, the cladding temperature will rapidly increase. Both the magnitude and the rate of temperature increase are dependent on the local power and coolant conditions. It is postulated that the post-CHF temperature transient will lead to one of four possible situations:

1. The cladding will attain a stable elevated temperature with little or no detrimental short-term effects on the cladding,
2. The cladding will attain a stable elevated temperature where metal-water reaction ultimately leads to brittle-fracture of the cladding,
3. The cladding will plastically rupture, or
4. The cladding will melt.

Because of the axial variation of local conditions (power, heat transfer, etc) it is possible that several of these situations could exist at various axial locations on the same fuel rod.

If the cladding integrity is lost, as will be the case for Situation 2, 3, and 4, fuel-coolant interactions and pressure disturbances may occur. Although the results from cladding failure of a few fuel rods may not be severe in a reactor environment, the possibility that the consequences of a PCM accident may initiate rod-to-rod cladding failure propagation, makes the PCM accident a reactor safety concern.

The first test series to be conducted in PBF is the simplest case of overpower, entitled PCM-20, consisting of a controlled sequence in which the power level in the fuel is slowly increased while the coolant flow is maintained at a fixed level. The test sample used in this test series will be a single PWR-type fuel rod positioned within a central test space within the PBF driver core.

In the PCM-20 tests, the behavior of single unirradiated PWR-type fuel rods will be evaluated under actual power-cooling mismatch conditions. These test fuel rods will be instrumented and their dynamic behavior will be determined under various degrees of imbalance between power and cooling. The experiments will be carried out within the controlled environment of the PBF test space.

Standard Problem

Development of models which predict the entire course of fuel rod behavior during the PCM-20 accident sequence is presently underway at Aerojet Nuclear Company for the AEC. The models when completed will describe the following in sequential order: (1) the status of the fuel rod at the beginning of the accident (including all the important effects of burnup); (2) the thermal and mechanical responses as the fuel rod responds to overpower (rise in temperature, CHF, post-CHF, thermal stresses, failure, meltdown); (3) eventual interaction of failed fuel rod materials and coolant; and (4) propagative and large-core processes.

At the present time, modeling is concentrating on Areas 1 and 2 above. The initial PCM-20 tests also concentrate in this area by obtaining data on fuel rod behavior up to the time of failure.

Thus, the Standard Problem proposed is one which will allow interested parties an opportunity to predict the prefailure behavior of a single fuel rod. The predictions can be made using any methods, codes, or proprietary data available and the results will be compared to the data arising from the PBF PCM-20 tests, particularly test number 3-3, as shown later.

Input Data

Input data for calculations of PCM-20 test data includes test hardware specifications and final test system conditions. Most of this information is available in the Detailed Test Plan Report (DTPR) for PCM-20 presently in draft form and available soon to industry. Additional needed information, if any, can be obtained directly from ANC. The DTPR will also show the relation between the test anticipated for this Standard Problem and the remaining tests which comprise the complete PCM-20 test series.

For purposes of preliminary review, the following pages have been taken from the DTPR. They show: the overall testing plan for PCM-20;

how the tests will be conducted; the relationship of test number 3-3 (to be used for this Standard Problem) to the remaining tests; Schematics of the hardware; anticipated measurements and instruments used to obtain the measurements; computer codes being used by ANC to predict test results; and examples of test predictions. It should be noted that the information on these pages is still preliminary and subject to change.

III. TEST PLAN

This chapter presents a description of the specific tests planned for Test Series PCM-20. The tests are designed to provide experimental data needed to evaluate and further develop analytical models as described in Chapter II. In addition, the proposed single rod tests will provide baseline data required to effectively plan, conduct and evaluate subsequent fuel rod cluster tests under power-cooling-mismatch conditions. Detailed descriptions of hardware and instrumentation, and pretest predictions of expected results are contained in Chapters IV and V respectively. The tests are presented in the order of expected conduct, however, the sequence may be varied if required on the basis of test data obtained.

1. INTRODUCTION

All tests will be conducted on fuel rods contained within the PBF inpile tube, which is centrally located in the driver core and is a part of the experimental loop system (see Appendix A for an overall description of the PBF). Loop coolant pressure and temperature will be constant for all tests, while flow rate through the test assembly will be an experimental variable. The test rods will be typical of PWR design and will contain previously unirradiated (zero burnup) fuel. Except for one 9-rod cluster calibration test, all tests will be conducted on single rods.

The planned tests are divided into 7 groups, comprising a total of at least 22 tests, as shown in Figure 3-1. The key tests that provide the bulk of the data for model evaluation and development are included in test groups 3, 4, and 5; the other four test groups are for calibration and scoping purposes. Test groups 1 and 7 are power calibration tests on single and 9-rod clusters, respectively. Test group 2 is a CHF scoping test to determine the gross temperature and mechanical history of a fuel rod following CHF. Test group 6 is test designed to evaluate the effect on the thermal and mechanical behavior following CHF of reducing the initial internal gas pressure within the fuel rod from 550 psi to atmospheric pressure. Test groups 3, 4, and 5 comprising 6 tests each, will be conducted at 3 flow rates, 1.0, 1.75 and 2.5 $\times 10^6$ lb/hr-ft^2, respectively.

Flow rate variations provide a convenient means of markedly affecting the behavior of

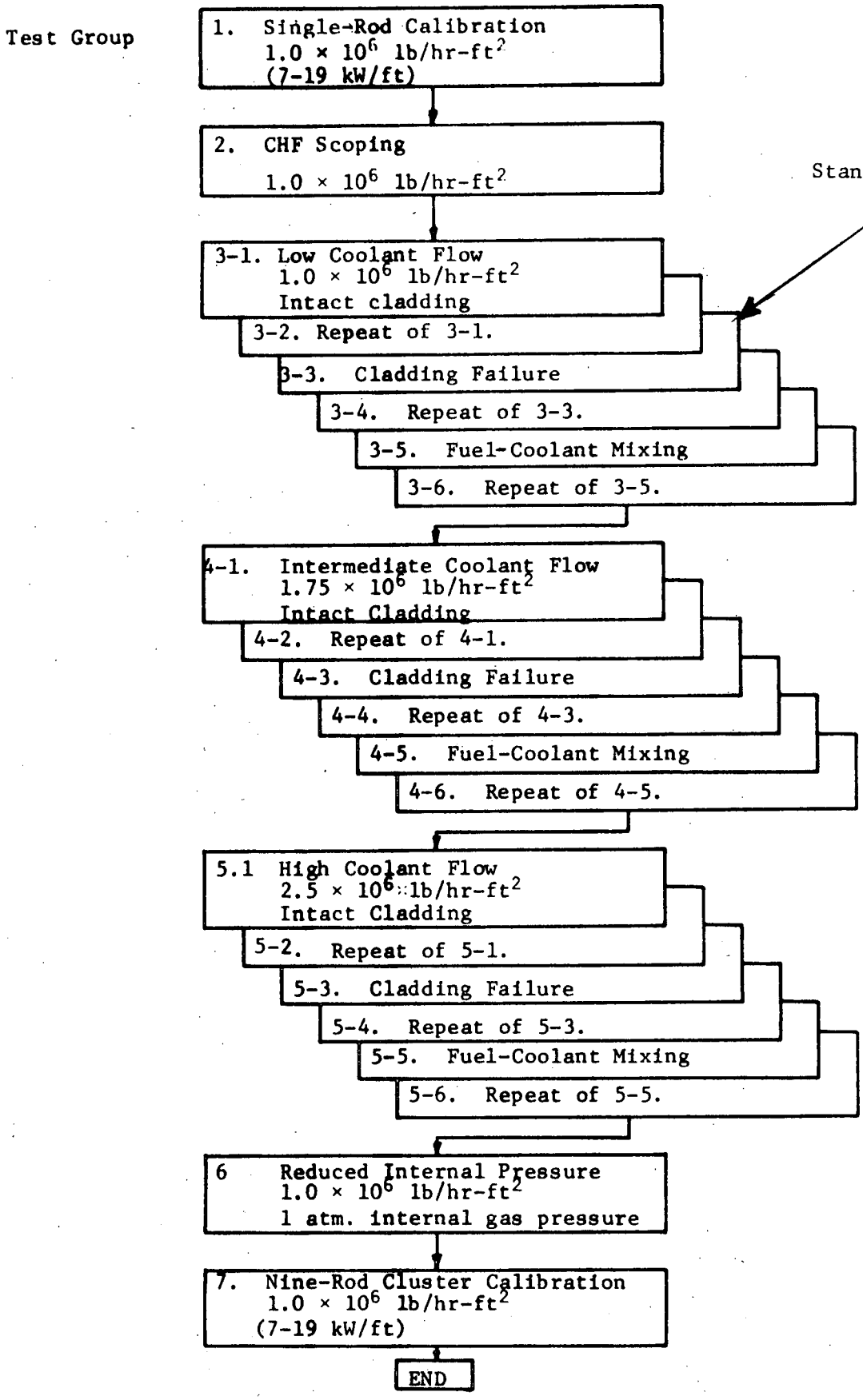

Fig. 3-1. Sequential order of PCM-20 tests.

the test rods for model evaluation purposes. The effects of varying the flow rate and the rationale for the three flow rates chosen are discussed in Section 4.2 of Chapter V.

Within each of test groups 3, 4 and 5, an attempt will be made to provide three distinct termination points following CHF, thus allowing additional information to be obtained from posttest examination of the test rods. Within each group of six tests, the first set of two tests will be terminated prior to the loss of cladding integrity. The second set of two tests will be terminated prior to fuel melt-through to the coolant. The third set of two tests will be terminated after fuel has melted through to the coolant and had sufficient time to undergo reaction with the coolant.

All tests will be conducted by increasing the test rod(s) power in increments to that level required to meet test objectives. Each power level below CHF will be held constant for at least 10 minutes to attain equilibrium temperature conditions in the coolant and test rod. Each power increase will not be more than 1 kW/ft peak linear rod power at a rate of 1 kW/ft-min when near CHF. The expected power history for each test group is shown in Figure 3-2. The procedures for increasing the power are based on PWR operating limits. The calculated relation between the test rod peak linear power and the PBF driver core power is shown graphically in Figure 3-3. These results will be adjusted on the basis of experimental data obtained during calibration tests.

The following descriptions of each test group include brief statements of purpose, test conditions, operating sequence, and required instrumentation.

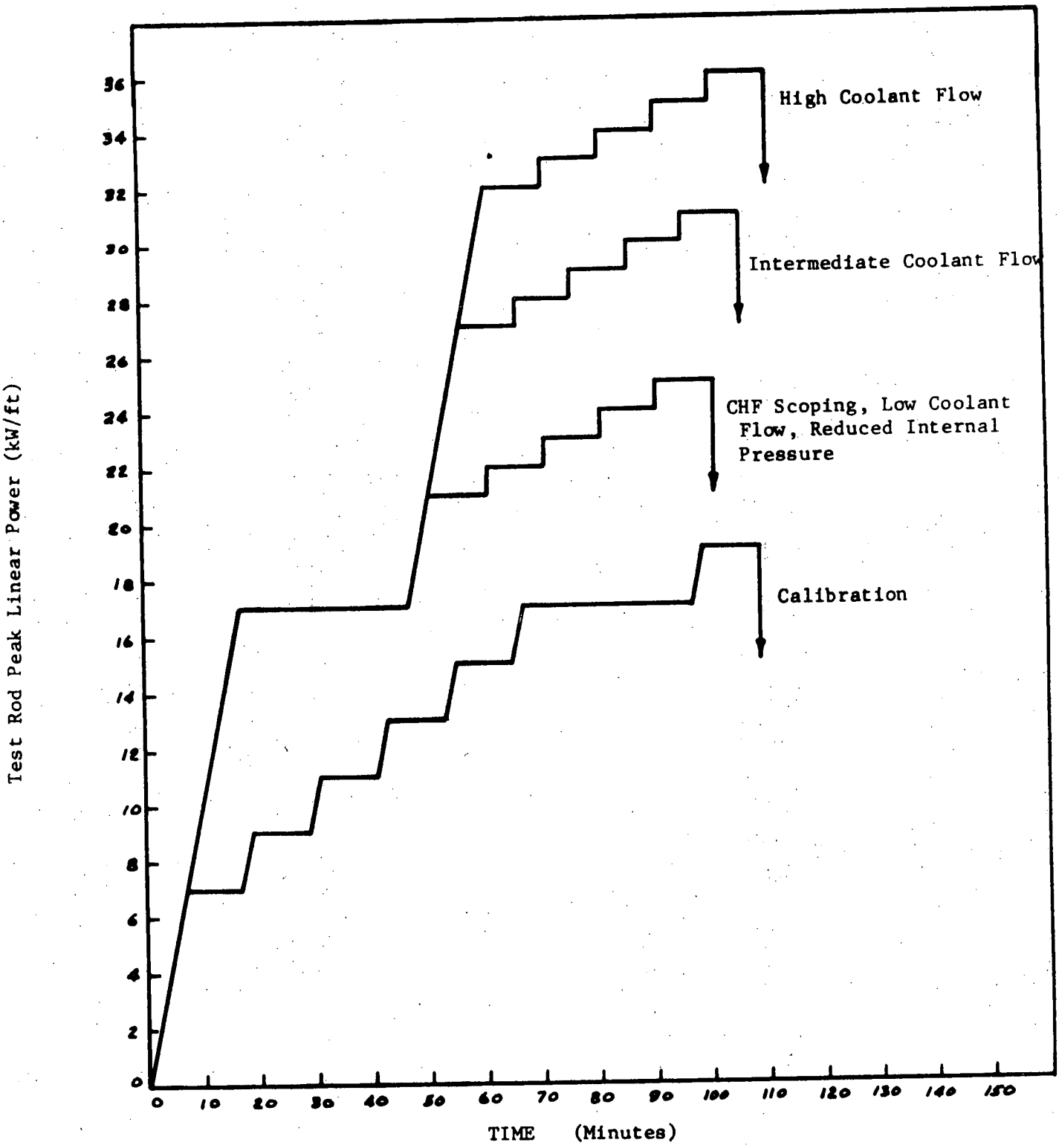

Fig. 3-2 Power history schematic for PCM-20 tests.

2.3 Test Group 3 - Low Coolant Flow

This test group is comprised of six tests with a flow rate of 1×10^6 lb/hr-ft^2 for the purpose of deriving details of the behavior of a test fuel rod following CHF at this flow rate. The tests are divided into three sets of two tests each. The termination point is varied for each set for posttest evaluation purposes.

In all tests, the initial loop conditions will be 2200 psia, a flow rate of 1×10^6 lb/hr-ft^2, and an inlet temperature of 620°F (644 Btu/lb). The test rod power will be brought up to a steady state peak linear power density of 17 kW/ft on a one kW/ft-min. ramp. This steady state level will be held for a minimum of 30 minutes to allow partial restructuring of the fuel. The test rod peak power density will then be increased on a one kW/ft-min. ramp to 21 kW/ft. The power level will then increase in one kW/ft increments until CHF occurs. All steady state levels will be held constant for a minimum of ten minutes. CHF is expected to occur at about 25 kW/ft peak (21 kW/ft at the axial point of initial CHF) and will be determined approximately during the scoping test (Section 2.2).

The first set of two tests in this group will be terminated after cladding melting but prior to fuel melt-through to the coolant. This will be accomplished either by terminating after a preset time determined during the scoping test, or by terminating on the basis of on-line observations of cladding surface temperature, internal fuel rod pressure, and/or pressure differential across the test assembly.

The third set of two tests will be terminated after fuel has melted through to the coolant and has had sufficient time to undergo mixing and possible reaction with the coolant. Termination will be accomplished on the basis of on-line observation of test instruments, possibly in combination with level trips on the dynamic pressure transducers.

In planning the three termination points, it was assumed that the cladding temperature would continue to increase following CHF until cladding melting occurred. Recent calculations including radiant heat transfer

predict, however, that the cladding temperature levels off below cladding melting following CHF (see Chapter V). The results of the CHF scoping test will allow this prediction to be evaluated. In the event cladding melting does not occur during the scoping test, the power will be incrementally increased following CHF during the second and third sets of tests in this group to effect cladding melting and fuel-coolant mixing, respectively. The incremental power increases will not exceed 1 kW/ft with at least ten minutes between each step.

Test hardware and instrumentation for these tests will be identical to that used for the scoping test (Section 2.2).

1.2 Single Rod Test Hardware

All single rod tests except the calorimeter calibration test will use the same hardware within the IPT. The design is the same as the calorimeter hardware except for the size of the shroud about the test rod. The single rod tests will have a 304 stainless steel shroud that is 1.000 inch OD with a 0.120 inch wall thickness, resulting in a cross-sectional flow area of 0.325 square inches[a]. A schematic of the single rod test hardware is shown in Figure 4-6.

[a] The unit cell flow area appropriate to a PWR having the same fuel rod dimensions is 0.177 square inches. However, calculations show that CHF in the PCM-20 tests will occur at the same normalized location as CHF in a 12-foot PWR fuel rod under operating conditions.

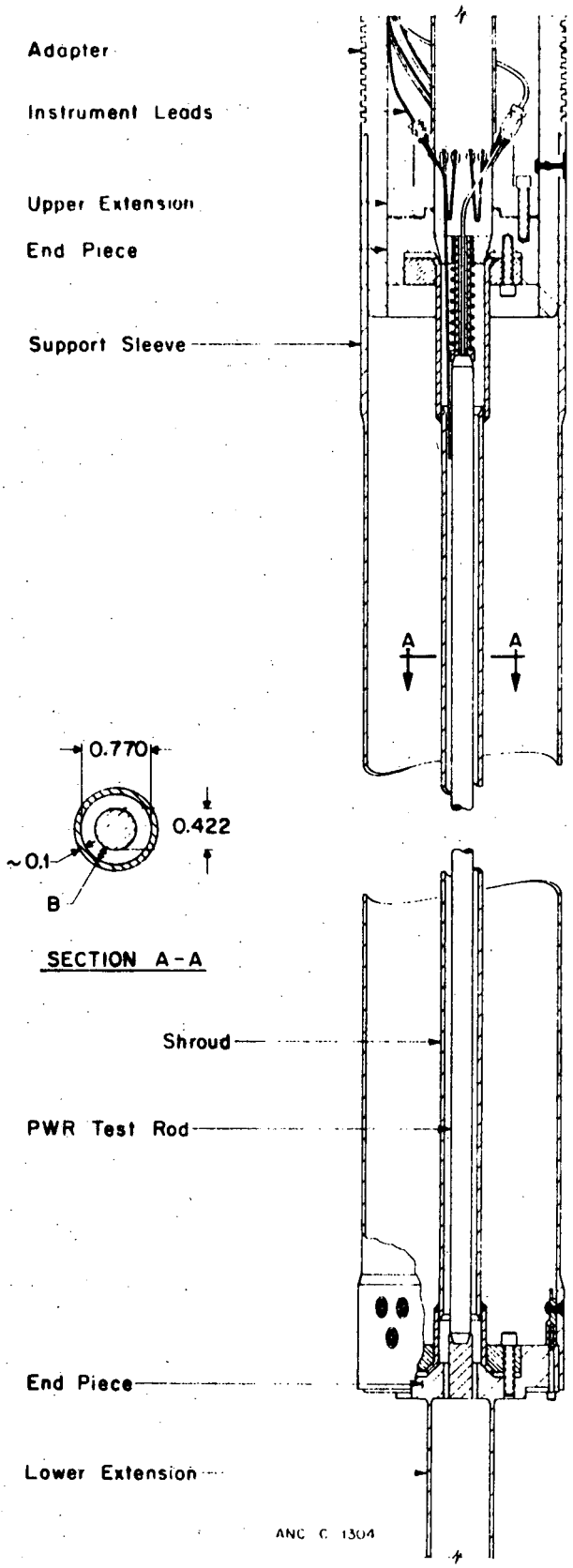

Figure 4-6. Single rod test hardware.

TABLE IV-1

PWR TEST FUEL ROD DATA

Fuel

Ceramic grade, dished and sintered uranium dioxide pellets

stack length (inches)	36.000 ± .065

Type A (20% Enriched Nominal)

Enrichment (w/o U-235 of total U)	19.87 ± .03
Uranium content (w/o U)	88.1 ± .2
Density (g/cc)	10.23 ± .04
Pellet Diameter (inch)	0.3660 ± .0005
Pellet Length (inch)	0.61 ± .01
Moisture (ppm)	7.4 max
Total impurities (ppm)	<364
O:U ratio	2.002 ± .002

Type B (35% Enriched Nominal)

Enrichment (w/o U-235 of total U)	34.87 ± .03
Uranium content (w/o U)	88.0 ± .2
Density (g/cc)	10.22 ± .03
Pellet Diameter (inch)	0.3660 ± .0005
Pellet Length(inch)	0.61 ± .01
Moisture (ppm)	7.1 max
Total impurities (ppm)	<338
O:U ratio	2.001 ± .001

Type C (93% Enriched Nominal)

Enrichment (w/o U-235 of total U)	93.15 ± .02
Uranium content (w/o U)	88.0 ± .1
Density (g/cc)	10.14 ± .05
Pellet Diameter (inch)	0.3660 ± .0005
Pellet Length (inch)	0.61 ± .01
Moisture (ppm)	2.7 max
Total impurities (ppm)	<382
O:U ratio	2.001 ± .001

Cladding Tube

Zirconium alloy manufactured to ASTM B 353-69, Grade RA-2, 50% coldworked and stress relieved, nominal values.

Inside diameter (inch)	0.374
Wall thickness (inch)	0.024
Yield strength (0.2% offset, psi)	81,000
Tensile strength (psi)	108,000
Elongation (%)	18
Hardness (R_B)	96

TABLE IV-1 (contd)

End Cap Rod Stack

Zirconium alloy manufactured to ASTM B 351-67, Grade RA-1, annealed, nominal values.

Yield strength (0.2% offset, psi)	49,500
Tensile strength (psi)	77,100
Elongation (%)	25
Hardness (BHN)	176

Compression Springs

Oil tempered chromium-vanadium alloy spring steel manufactured to ASTM A 231-68, nominal values.

Wire diameter (inch)	.041
Tensile strength (psi)	296,000
Spring rate (lb/inch)	6.4-8.7
Spring outside diameter (inch)	.355
Free length (inch)	2.375
Total number coils	17

Insulating End Spacers

Coors Porcelain Co., ceramic grade sintered alumina, nominal values.

Density (grams/cc)	3.90
Compressive strength (psi)	362,000
Length (inch)	.250
Diameter (inch)	.365

Fuel Rod

Nominal values.

Overall length (inch)	39.9
Outside diameter (inch)	.422
Active fuel length (inch)	36
No. fuel pellets	59

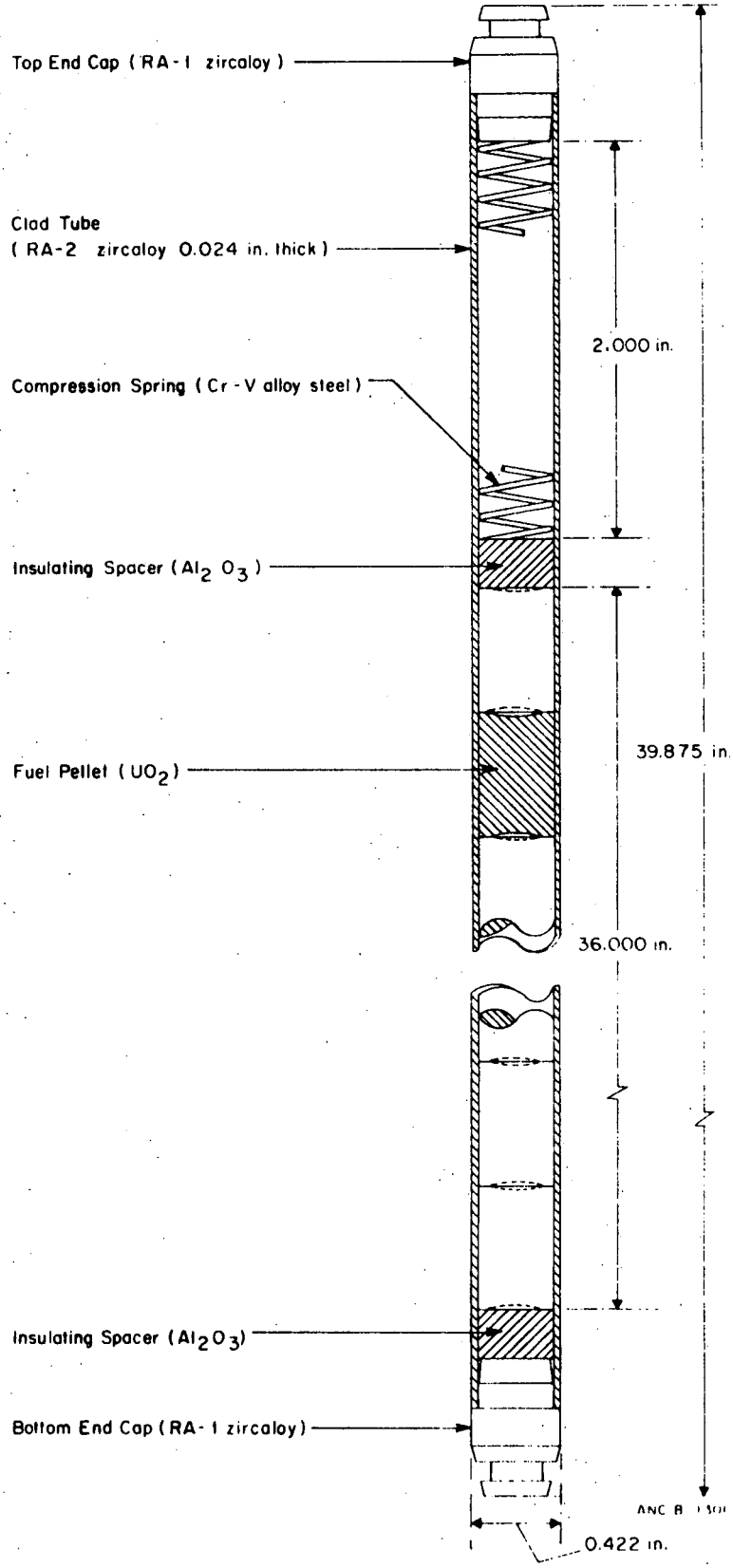

Figure 4-8. Schematic of PWR test fuel rod.

TABLE IV-2

PRETEST MEASUREMENTS FOR PCM-20 TEST SERIES

A. The following material properties are taken from the latest available literature source.

1. Thermal conductivity of UO_2
2. Modules of elasticity of UO_2
3. Thermal expansion of UO_2
4. Modules of elasticity of cladding
5. Coefficient of thermal conductivity of cladding
6. Coefficient of thermal expansion of cladding
7. Thermal emissivity of cladding

B. The following measurements are supplied by the fuel fabricator.

1. Density of UO_2
2. Tensile strength of cladding
3. Yield strength of cladding
4. Percent elongation of cladding
5. Hardness of cladding
6. Percent cold work of cladding
7. Surface roughness of cladding
8. Free void volume of test rod
9. Internal gas pressure of test rod
10. Weight of UO_2 in test rod
11. Enrichment of UO_2
12. Impurities in UO_2
13. Chemical composition of cladding

C. The following measurements are made in Aerojet Nuclear Company facilities.

1. Grain size and distribution in the UO_2 pellets
2. Grain size and distribution in the cladding
3. Dimensions of the test rod
4. X-ray, gamma, and neutron radiography of the test rod
5. Geometry of the test
6. Photographs of test rod, test cluster, and instrumentation

TABLE IV-3

DYNAMIC MEASUREMENTS FOR PCM-20 TEST SERIES

Measurement	Method	Instrumentation Type	Instrumentation Location
. Test power density	Calibrated to reactor power	Reactor instrumentation-neutron chambers	Chambers located outside PBF core
	Calorimetry and power distribution		
	Coolant Mass flow	Refer to Item 4	Refer to Item 4
	Coolant ΔT	Two resistance thermometers	Upstream (below) & downstream (above) test fuel
	Relative power	Cobalt wires and gamma scan of test rods	In test assembly
. Inlet coolant enthalpy	Coolant temp. (in conjunction with pressure)	Chromel-Alumel thermocouple	In coolant flow upstream of (below) test fuel
. Coolant pressure	Pressure transducer	Bonded strain gauge transducer	In coolant channel downstream of (above) test fuel
. Coolant mass flow through test	Flow velocity (in conjunction with coolant density)	Turbine flow velocity	In coolant channel upstream of (below) test fuel
. Coolant pressure differential across test hardware	Measure difference in pressure	Pressure differential gauge	Lead tubes, one located at bottom and one at top of test cluster
. Occurrence of CHF	Increase in cladding surface temp. at steady power	W-5% Rh - W-10% Rh thermocouples	Surface TC in the region of predicted CHF
. Time-Temp. response of fuel and cladding	Cladding temp.	Same instrument as Item 6	Same location as Item 6
	Fuel temp.	High Temperature Ultrasonic Thermometer	Axial centerline of test fuel
. Time of cladding failure	Detect change in fuel-rod internal pressure	Bonded strain gauge pressure transducer and/or strain gauge	Penetration at upper end of fuel rod Welded to fuel rod spring plenum

TABLE IV-3 (contd)

Measurement	Method	Instrumentation	
		Type	Location
Pressure pulse(s) generated by fuel cladding failure	Pressure transducer in coolant flow	Bonded strain gauge transducer	Two transducers of different ranges downstream of (above) test fuel. (One is same as Item 3
Difference in the fuel rod internal and the external pressure	Difference between two absolute pressures	Item 3 and Item 9	Refer to Item 3 and Item 9

TABLE IV-6

INSTRUMENTATION REQUIREMENTS AND CAPABILITIES

Measurement	Requirement	Instrument	Instrument Capability[a]
Differential Pressure Across Test Assembly	Accuracy: ±0.5 psi Range: 0-15 dpsi Time Response: 0.1 sec	Schaevitz Model PT-70 Differential Pressure Transducer[b]	Accuracy: ±0.15 psi Range: 0-25 dpsi Time Response: <0.1 sec
Coolant Pressure at Outlet of Test Assembly	Accuracy: ±2% Range: 0-2300 psi Time Response: 0.1 sec	Norwood Pressure Transducer Model 70007-2[c]	Accuracy: ±1% full scale Range: 0-3000 psi Time Response: ~15 μsec
Dynamic Pressure in Flow Field	Accuracy: ±10% Range: 0-7500 psi Time Response: 20 μsec	Norwood Pressure Transducer Model 70007-5[c]	Accuracy: ±1% full scale Range: 0-10,000 psi Time Response: ~15 μsec
Fuel Rod Internal Pressure	Accuracy: ±5% Range: 100-5000 psi Time Response: 0.1 sec	Norwood Pressure Transducer Model 70007-5[c]	Accuracy: ±1% full scale Range: 0-5000 psi Time Response: ~15 μsec
Differential Coolant Temperature Across Test Assembly	Accuracy: ±0.25°F Range: 0-50°F Time Response: 5 sec	Platinum Resistance Thermometer Model R-14.3-96D100[d]	Accuracy: ±0.2°F Range: 0-100°F Time Response: 3 sec[e]
Inlet and Outlet Coolant Temperature	Accuracy: ±2% Range: 500-700°F Time Response: 0.1 sec	Aeropak Chromel-Alumel Thermocouple Model 040-2M-AKS-34[d]	Accuracy: ~±3/8% full scale Range: 0-2000°F Time Response: < 0.1 sec
Cladding Temperature			
High Temperatures	Accuracy: ±3% Range: 800-3300°F Time Response: 0.1 sec	High Temperature Thermocouple (W-5 Re/W-26 Re) Model T-50031-12-120 and T-50031-28-120[d]	Accuracy: ±1% full scale Range: 0-3500°F Time Response: <0.1 sec
Low Temperatures	Accuracy: ±1% Range: 600-800°F Time Response: 0.1 sec	Aeropak Chromel-Alumel Thermocouple Model 040-2M-AKS-34[d]	Accuracy: ±3/8% full scale Range: 0-2000°F Time Response: <0.1 sec

TABLE IV-6 (contd)

Fuel Centerline Temperature			
Primary Instrument	Accuracy: ±100°F Range: 0-5200°F Time Response: 1 sec	High Temperature Ultrasonic Thermometer[f]	Accuracy: ±50°F Range: 0-5400°F Time Response: 1 sec
Secondary Instrument	Accuracy: ±100°F Range: 0-4900°F Time Response: 1 sec	High Temperature Thermocouple (W-5 Re/W-26 Re) (Model not determined at present)	Accuracy: ±50°F Range: 0-4900°F Time Response: 0.5 sec
Coolant Flow			
Single Rod Assembly	Accuracy: ±2% Range: 10-100 gpm Time Response: 1 sec	Turbine Flowmeter[f]	Accuracy: ±1.5% Range: 0-100 gpm Time Response: 1 sec
Full Coolant Flow	Accuracy: ±2% Range: 100-800 gpm Time Response: 1 sec	Turbine Flowmeter[f]	In design
Time of Failure	Accuracy: ±15% Range: 0-600 μ in./in. Time Response: 0.1 sec	Strain Gauge Model MG125[g]	Accuracy: ±10% Range: 0-6000 µin/in. Time Response: 0.1 sec

[a]Accuracies shown represent the capabilities of the instruments only. The data acquisition and recording system that processes the data has the capability of responding to within ±1% of the input signal. Where greater precision is needed to meet measurement requirements, direct recording will be used.
[b]Schaevitz Engineering, Pennsauken, New Jersey.
[c]Precise Sensors Co., Monrovia, California.
[d]ARI Industries, Franklin Park, Illinois.
[e]For a 63% response to a step change.
[f]Built by ANC, I&CE Branch.
[g]Microdot Inc., City of Industry, California.

TABLE II-1

CONTRIBUTION OF PCM 20 TO CALCULATIONAL TECHNIQUES

Major Area of Calculational Uncertainty	Codes	Principal Uncertainty Affecting Calculational Results	Measurements to be Made in PCM-20	Measurement Accuracy Requirements[a]
1. Fuel Temperature Distribution ±500 °F	HEAT-I TOODEE THETA1-B GAPCON	Gap h (initial) ±30-80% Power ±10% UO_2 conductivity ±10%	Fuel Centerline Temperature Cladding Surface Temperature Internal Fuel Rod Pressure Power Coolant Temperature, Pressure, Flow Posttest Examination	±100°F ±1% below CHF ±5% ±10% ±2% ---
2. Fuel Temperature Distribution after CHF to Cladding Failure ±500 - 1000°F	HEAT-I TOODEE GAPCON	Gap h (initial) ±30-80% Cladding Temperature ±5-20% Film Coefficient ±15-20% Power ±10%	Fuel Centerline Temperature Cladding Surface Temperature Power Coolant Temperature, Pressure, Flow Internal Fuel Rod Pressure Posttest Examination	±100°F ±3% ±10% ±2% ±5% ---
3. Clad Temperature after CHF ±5% ±20% above 2000°F	HEAT-I TOODEE THETA1-B Baker-Just (M/W)	Film Coefficient ±15-20% Gap h (transient) ±80+% Metal Water Reaction Rate ±50% Geometry Changes Power ±10%	Cladding Surface Temperature Coolant Temperature, Pressure, Flow Fuel Centerline Temperature Internal Fuel Rod Pressure Oxidation of Cladding (posttest) Power	±3% ±2% ±100°F ±5% ±25% ±10%
4. Cladding Deformation ±50%	AXPLAS CYGRO	Cladding Temperature Distribution ±3-20% Cladding Internal Pressure ±25% Materials Properties ±15% Fuel Cladding Interactions ---	Cladding Surface Temperature Fuel Rod Internal Pressure Fuel Centerline Temperature Coolant Temperature, Pressure, Flow Pretest Characterization Posttest Examination	±3% ±2% ±100°F ±2% --- ---
5. Post Fuel Rod Failure Effects	SPIRT Undeveloped Models	Fuel Temperature Dist. at Failure Pressure Pulse Generation Fuel Dispersal Rate Fuel Particle Size Fuel Coolant Heat Transfer Vapor Formation	Fuel Centerline Temperature Pressure Pulse in Coolant Posttest Particle Size Distribution	±100°F ±10% ---
6. Effects of Irradiation	CYGRO GAPCON	Fuel Geometry Changes Materials Properties Changes	These tests will be with unirradiated fuel, thus the tests will provide baseline data for determining the effects or irradiation in future tests with pre-irradiated or simulated irradiated fuel.	

[a] These measurement requirements have been estimated from limited sensitivity studies of the various codes with consideration of the state-of-art of the variou measurement techniques.

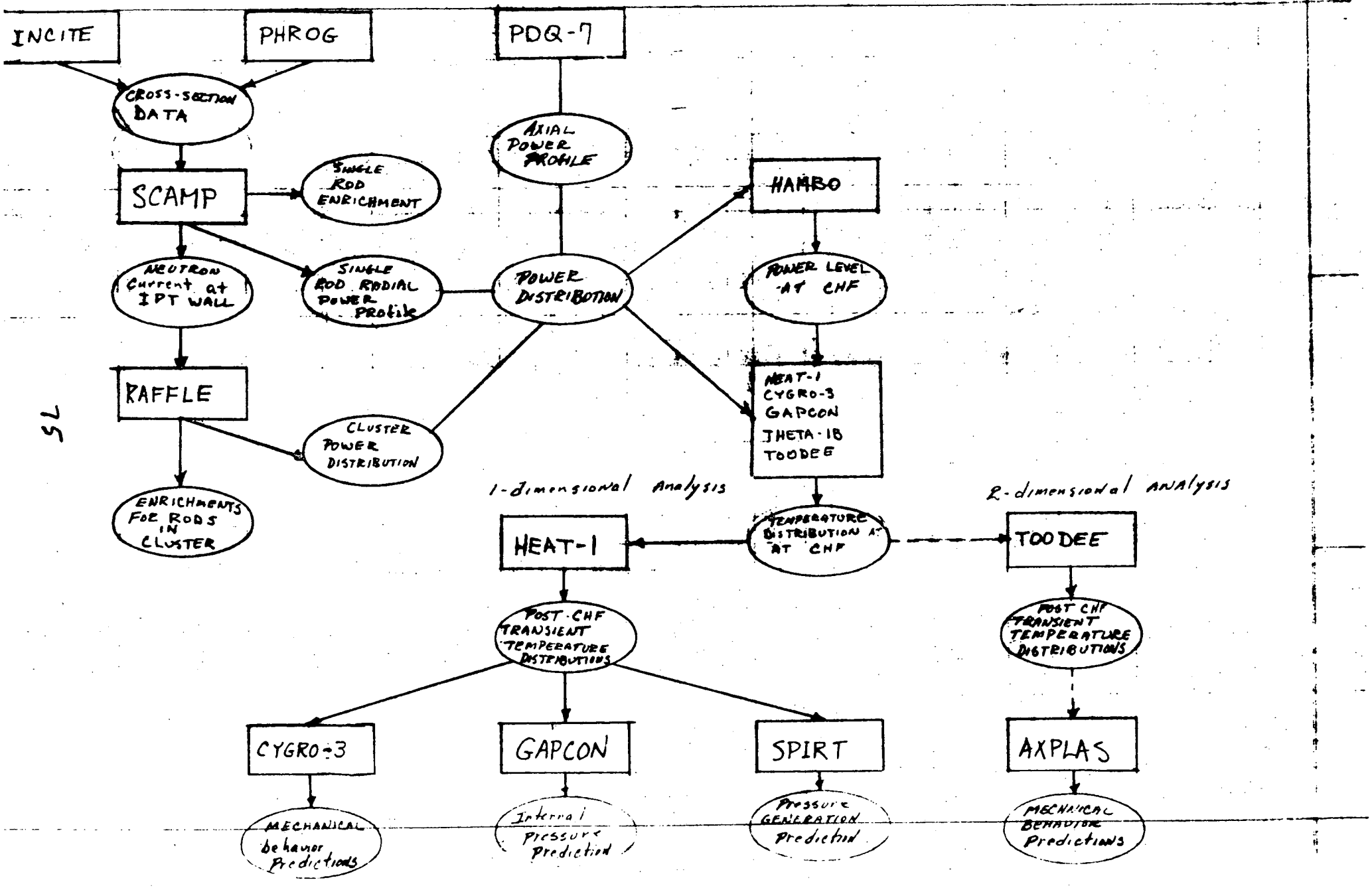

5-1 OVERALL ANALYSIS

TABLE V-1

SUMMARY OF COMPUTER CODES USED IN ANALYSIS

OF PCM-20 TESTS

COMPUTER CODE	RESPONSE AREA	PROBLEM SOLVED	INPUT REQUIRED	OUTPUT
RAFFLE[16]	Neutronic	Steady-state, multigroup neutron transport equation in 2 or 3 dimensions. Solved using Monte Carlo method	Cluster geometry, material density, material cross-sections, external source currents	Spatially dependent multigroup fluxes, reaction rates, & neutron currents
SCAMP[17]	Neutronic	Steady-state, multigroup neutron transport equation in radial direction using S_n approximation	Multigroup cross-sections from PHROG & INCITE. Geometrical description	Spatially dependent multigroup fluxes, reaction rates & neutron currents
HEAT-1[18]	Thermal	One-dimensional, time-dependent heat conduction equation for a single fuel rod	Fuel rod geometry, temp. dependency of material properties power distribution & boundary conditions	One-dimensional temp. distribution in fuel and clad and surface heat flux
TOODEE[19]	Thermal	Two-dimensional, time-dependent, heat conduction equation in RZ, RΘ or XY geometry for a single fuel rod. Energy balance in coolant for single-phase fluid	Fuel rod geometry, temp. dependency of material properties, power distribution, initial coolant conditions, & boundary heat transfer conditions	Two-dimensional temp. distribution in fuel and clad, surface heat flux, single channel coolant temperature
THETA1-B[20]	Thermal-Hydraulic	Two-dimensional, time-dependent heat conduction equation in RZ geometry for a single fuel rod. Energy & mass balance in coolant for single and two-phase fluids	Fuel rod geometry, temp. dependency of material properties, power distribution, & initial coolant conditions	Same as TOODEE
AXPLAS[21]	Mechanical	Time-dependent (through temp. dependence), RZ two-dimensional code for deformation of UO_2 and cladding	Geom. description of fuel rod, temp distrib. in fuel rod, internal & external fuel rod pressures, temp dependent mat'l properties	Time-dependent fuel and cladding deformation
CYGRO-3[22]	Mechanical	One-dimensional code for deformation of UO_2 and cladding. Includes empirical relationships for known effects of burnup	Same as above, except power history in fuel rod is required since CYGRO calculates the one-dimensional temp. distribution	One-dimensional (radial) time-dependent fuel and cladding deformation
HAMBO[23]	Hydraulic	Steady-state, two-dimensional subchannel hydraulic analysis of a fuel rod cluster assembly	Cluster geom., axial & radial heat fluxes, flow & friction correlations & subchannel mixing & CHF correlations, spacer pressure drop correlations	Local values for coolant flow rate, enthalpy, quality, press., density, void fraction, & slip rato. Predicts location of CHF
GAPCON[24]	Thermal	One-dimensional, steady-state heat conduction equation. Includes thermal expansion melting fuel restructuring, swelling and fission gas release.	Fuel rod geometry, temp. dependency of material properties, power distribution boundary conditions, plenum temperature and initial pressure.	One-dimensional steady state temperature distribution, internal pressure, gap conductance.
SPIRT[25]	Post failure hydraulic	One-dimensional, transient hydrodynamic equations with fuel-coolant heat transfer	Coolant conditions, fuel dispersal rates fuel particle size distribution and fuel temperature.	Time dependent pressure generation in the coolant.

TABLE V-5

CONDITIONS PREDICTED TO EXIST IN THE SINGLE-ROD TESTS AT TIME OF CHF

Coolant* Mass Vel. ($lb/hr\text{-}ft^2$)	Linear Power Density (kW/ft)		Estimated Reactor Power (MW)	Location of CHF (in.)	CHF $Btu/hr\text{-}ft^2$	Test Fuel Temp. (°F)		Maximum Cladding Surface Temp. (°F)	Coolant Quality (%)	
	Max.	Ave.				Max.	Ave.		At CHF	Outlet
1.0×10^6	24.7	17.9	15.8	21 to 23	6.72×10^5	4810	2620	660	1.8	6.6
1.75×10^6	30.9	22.4	19.8	19 to 21	8.42×10^5	5270	2920	661	0	1.9
2.50×10^6	35.2	25.5	22.5	19 to 21	1.02×10^6	5660	3120	662	0	0

*Enthalpy and pressure of the inlet coolant for this series of tests have been specified as 644 Btu/lb and 2200 psia respectively.

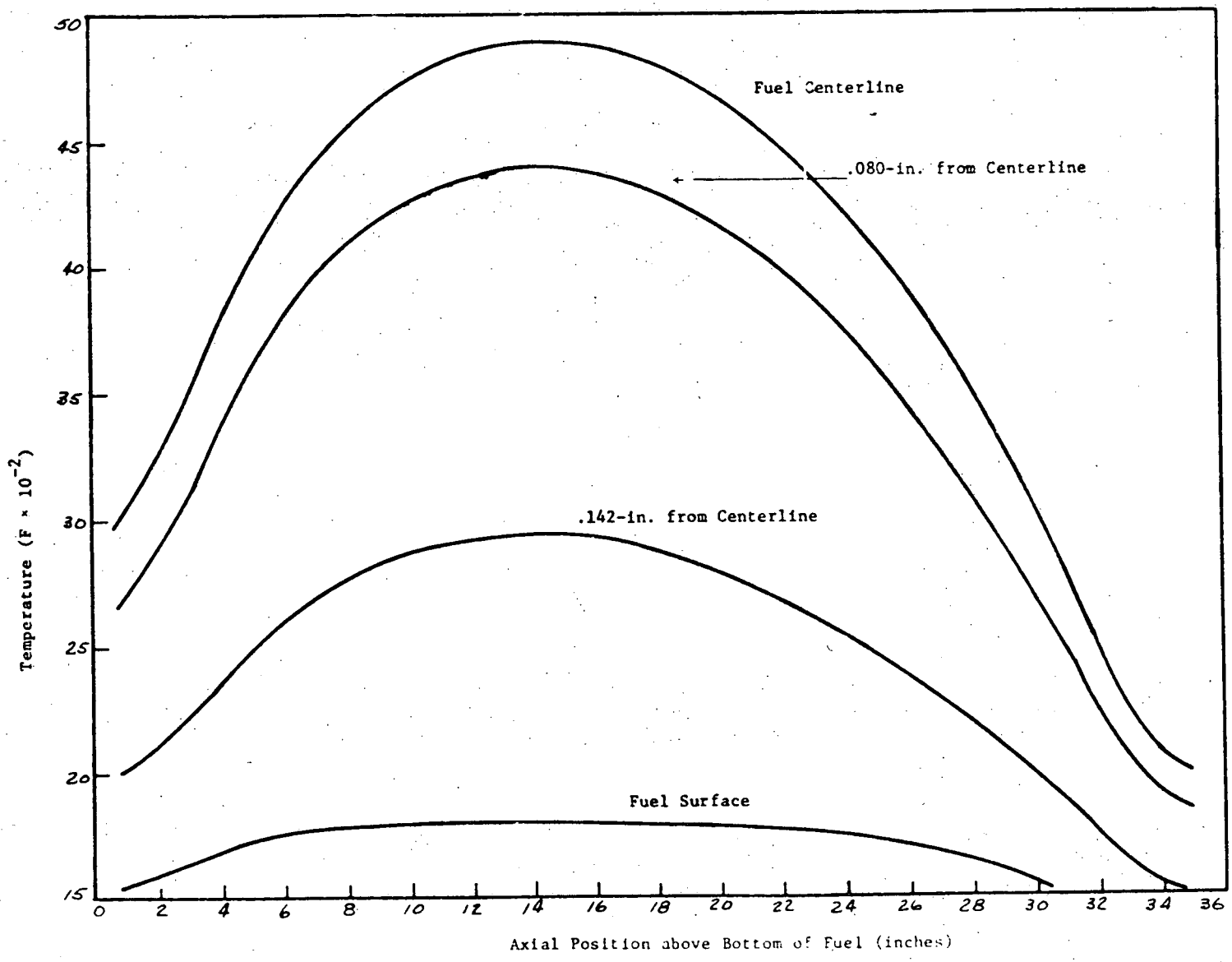

Fig. 5-17. Axial fuel temperature profiles at time of CHF for various radial nodes - single rod test worth 10^6 mass flow.

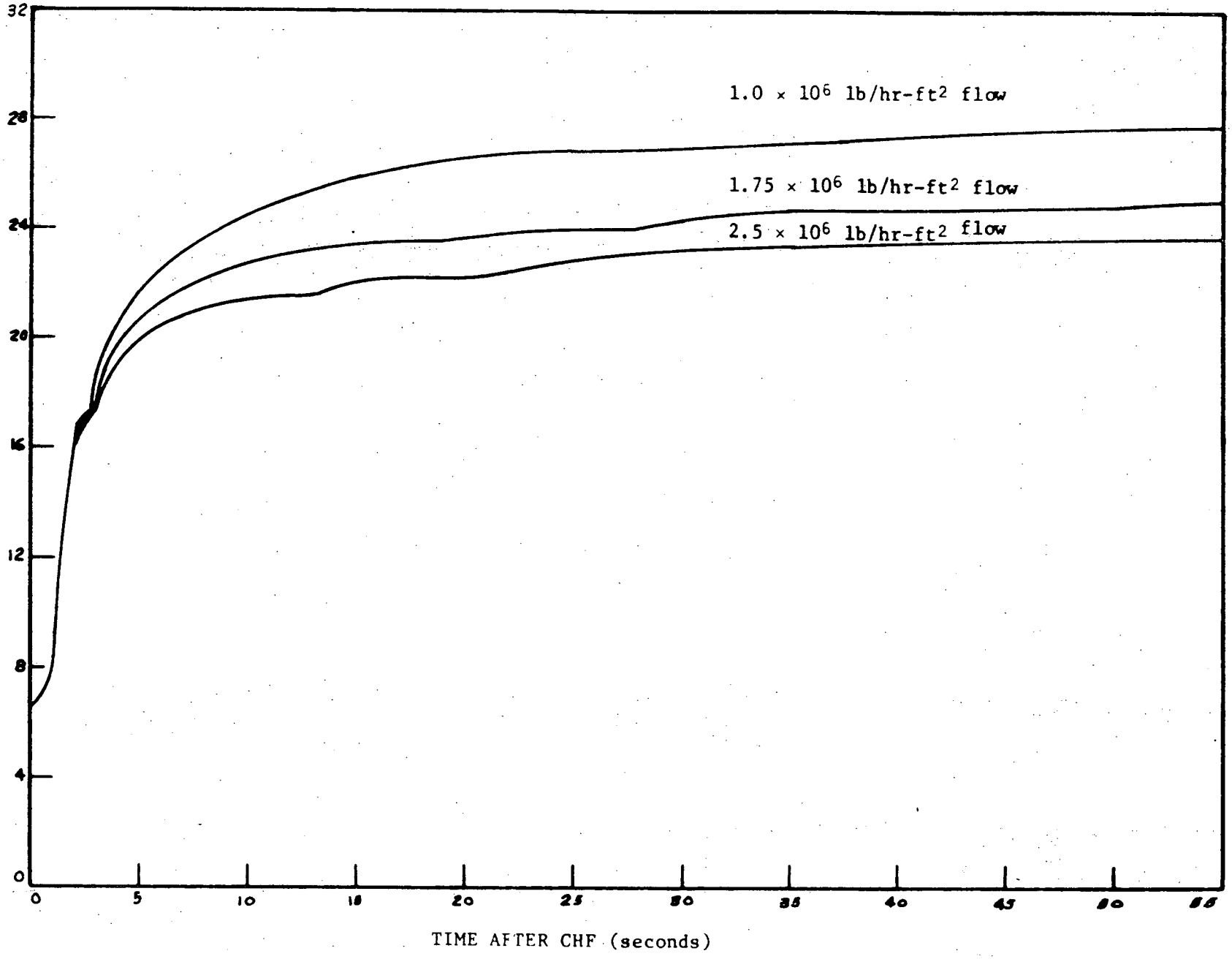

Fig. 5-27. Temperature history of cladding surface at CHF location.

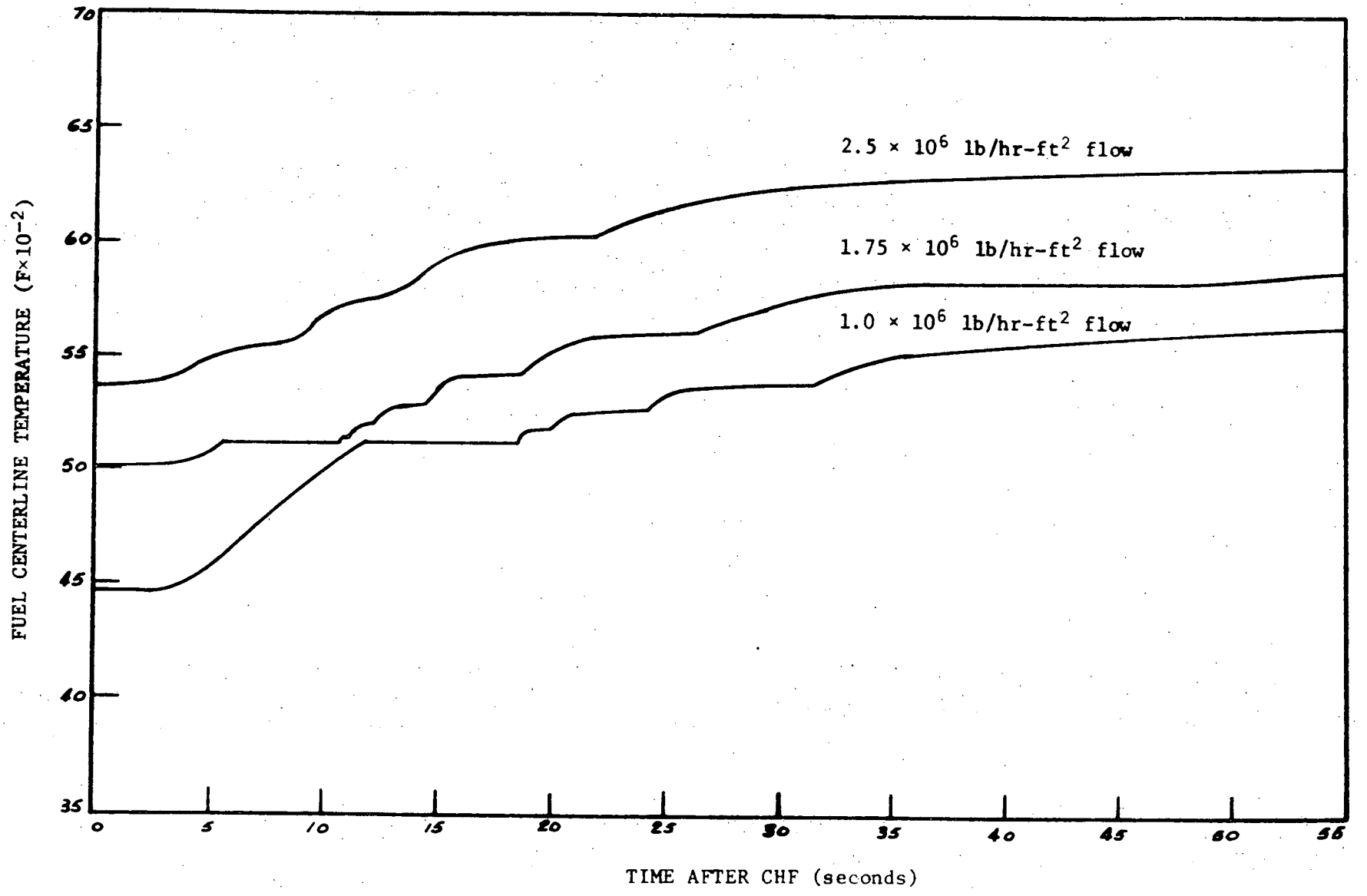

Fig. 5-28. Temperature history of fuel centerline at CHF location.